

Enhancement of the ferromagnetic order of graphite after sulphuric acid treatment

J. Barzola-Quiquia,¹ W. Böhlmann,¹ P. Esquinazi,^{1,*} A. Schadewitz,¹
A. Ballestar,¹ S. Dusari,¹ L. Schultze-Nobre,^{2,†} and B. Kersting²

¹*Division of Superconductivity and Magnetism, Institut für Experimentelle Physik II,
Universität Leipzig, Linnéstraße 5, D-04103 Leipzig, Germany*

²*Institut für Anorganische Chemie, Universität Leipzig, Johannisallee 29, D-04103 Leipzig, Germany*

We have studied the changes in the ferromagnetic behavior of graphite powder and graphite flakes after treatment with diluted sulphuric acid. We show that this kind of acid treatment enhances substantially the ferromagnetic magnetization of virgin graphite micrometer size powder as well as in graphite flakes. The anisotropic magnetoresistance (AMR) amplitude at 300 K measured in a micrometer size thin graphite flake after acid treatment reaches values comparable to polycrystalline cobalt.

PACS numbers: 81.05.uf,75.50.Dd

The possibility to trigger magnetic order in metal-free graphite by lattice defects or non-magnetic adatoms like hydrogen attracts the interest of basic and applied research fields¹. Recently published element specific x-ray magnetic circular dichroism (XMCD) measurements at the carbon K-edge in graphite samples^{2,3} clearly demonstrated that the reported magnetic order in metal-free graphite^{4,7} is not related to magnetic impurities. Published results from different groups indicate that vacancies⁵⁻⁷ and/or hydrogen^{3,8} can trigger this phenomenon, making the graphite structure the archetype of defect induced magnetism (DIM), a phenomenon that is being now found in nominally non-magnetic oxides^{9,10} as well as in Si-based samples¹¹ for example. In case of graphite magnetic order has been also achieved by a pulsed arc ignited between two graphite electrodes in ethanol¹². In general, however, the obtained yield remains small, partially because of the necessary delicate balance between a defect density of the order $\sim 5\%$, their positions and the lattice structure. For applications it is necessary therefore to find simpler methods to transform graphite in a magnet with reasonable high magnetization.

XMCD results in untreated as well as in proton irradiated bulk pyrolytic graphite provide clear hints for the influence of hydrogen atoms, especially a spin polarization splitting near the Fermi level³ in qualitative agreement with theoretical work published previously⁸. The aim of the here reported study was to find a simpler method to trigger magnetic order in graphite samples of mesoscopic size by including hydrogen at least in the near surface region without destroying its lattice structure or including further defects or contaminants. One possibility is to treat carbon with sulfuric acid leading to a hydrogen doping in the graphite structure.

Two kinds of graphite samples have been used in this work, namely an ultrapure graphite powder (impurity content < 1 ppm) consisting of platelet-like grains of average size $10 \times 10 \times 3 \mu\text{m}^3$ (see inset in Fig. 1) and a micrometer size graphite flake of thickness $\simeq 45$ nm (see inset in Fig. 3). The influence of the sulphuric acid on the powder has been measured using a superconducting quantum interferometer device (SQUID) and by trans-

port measurements in the case of the graphite flake, especially the anisotropic magnetoresistance (AMR) at different angles between field and current for fields applied parallel to the graphene planes of the sample.

Sample	H ₂ O	H ₂ SO ₄
S0	10 ml	10 ml
S1	-	20 ml
S2	20 ml	-
S3	5 ml	15 ml
S4	-	-

TABLE I. Powder samples prepared with different concentrations of sulphuric acid.

Each sample for the magnetization measurements was prepared mixing 100 mg of graphite powder into 20 ml of a liquid with sulphuric acid and water with a given concentration, see Table I. The suspension was continuously stirred at room temperature for 24 h. After stirring the obtained material was recovered by filtration and washed with distilled water to remove residual traces of acid and dried at 100 °C overnight for its characterization with the SQUID and infrared spectroscopy (IRS). For the SQUID measurements we used 10 mg of the prepared unpressed powder. For the IRS measurements we used the KBr method, i.e. 1 mg of the previously prepared graphite powder and 100 mg of KBr were mixed and pressed to form a tablet. The IR spectra were performed in transmission on a Perkin Elmer spectrometer. The micrometer size sample for the AMR measurements was obtained from a high oriented pyrolytic graphite (HOPG) sample by the rubbing method (for details see Ref. 13) and ohmic contacts were prepared using electron beam lithographic method.

Figure 1 shows the infrared absorption spectra of the graphite powder as received and after acid treatment. The comparison of the two spectra clearly shows the influence of the acid treatment. The increase in the intensity of the peak at 2943 cm^{-1} can be assigned to formed -C-H- stretching bands. Furthermore, in the region at

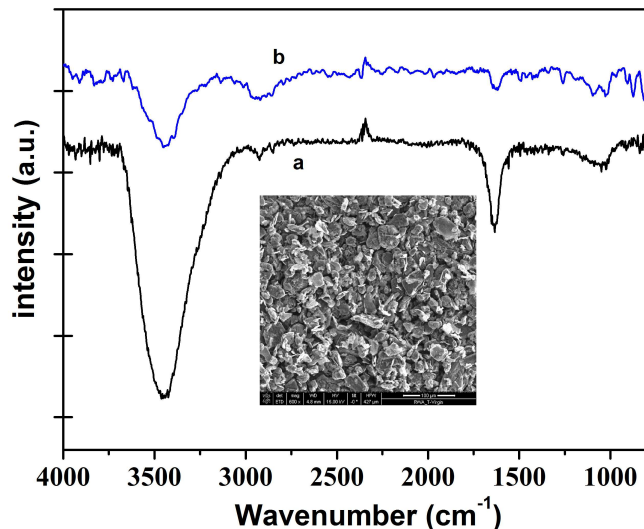


FIG. 1. Infrared absorption spectra of the graphite powder before (a) and after (b) acid treatment (sample S3). The inset shows a scanning electron microscope picture of the used powder. The scale bar indicates $100 \mu\text{m}$ length.

1650 cm^{-1} a medium band is observed, which generally belongs to C=C double bonds in aromatic rings¹⁴. The intensity of this stretching band decreases after the treatment with sulphuric acid demonstrating that partial hydrogen is embedded into the near surface region of the graphite structure. Similar results were obtained in Ref. 15 in activating processes of carbon black and carbon nanotubes with a mixture of concentrated $\text{H}_2\text{SO}_4 + \text{HNO}_3$ in an ultrasonic bath. The activation leads to the intensification of the band due to -OH vibration and to the appearance of many other bands such as those around 2920 cm^{-1} and between 1723 and 1090 cm^{-1} originating from vibration of oxygen functionalities. We note however, that according to the last XMCD results oxygen should not play any prominent role in triggering the magnetic order in graphite³.

Sample S2 was treated only with water using exactly the same procedure to check that it did not introduce any significant amount of impurities. The magnetic moment of the sulphuric acid alone and at room temperature did not show any ferromagnetic signals (not shown). Figure 2 shows the magnetization hysteresis loops at room temperature for the differently prepared powder samples after subtraction of the linear diamagnetic background. The magnetization was estimated taken the whole mass of the powder sample, which was in all cases 10 mg. The results presented in Fig. 2 reveal a clear influence of the acid on the ferromagnetic properties of the graphite powder. The small values of the obtained magnetization indicate that only the near surface region of the grains is affected by the acid treatment. From the XMCD results³ we may assume an intrinsic ferromagnetic magnetization at saturation $\gtrsim 15 \text{ emu/g}$. With the obtained satura-

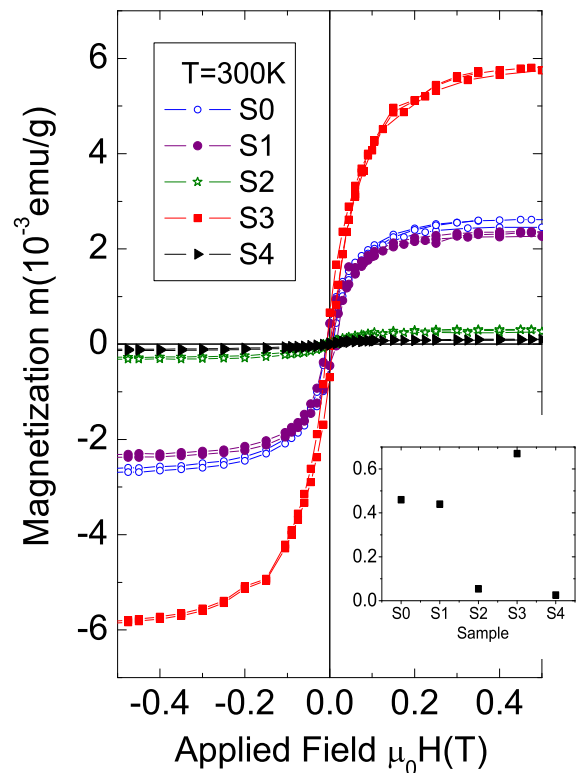


FIG. 2. Magnetization hysteresis loops for the differently prepared samples, see Table I. The inset shows the remanent magnetization in the same units for the different samples. The error in this measurement is less than the symbol size.

tion magnetization values for sample S3 and taking the average grain size we estimate an average magnetic near surface region of thickness $\lesssim 2 \text{ nm}$.

Figure 3 shows the magnetization vs. applied field for sample S3 before and after annealing it two hours in vacuum at 250°C . We observe a clear decrease of the ferromagnetic signal indicating that defects, in this case very probably hydrogen is related to the origin of the ferromagnetic enhancement.

An appropriate method to check the existence of ferromagnetism in a single micrometer small graphite sample is to measure the transport properties. In this work we concentrate ourselves to study the AMR, defined as the dependence of the magnetoresistance on the angle between the direction of the electric current I and the magnetic field H , in this case applied always parallel to the main area of the sample to keep any form-anisotropy or Lorentz-force contribution to the magnetoresistance invariant.

Figure 4 shows the magnetoresistance measured at a fixed field of 0.5 T as a function of the angle between the input current and the magnetic field. The graphite flake, see inset in Fig. 3, in its virgin state and at 300 K shows negligible AMR, whereas a clear AMR of $\simeq 0.1\%$ amplitude (defined between the maximum and minimum)

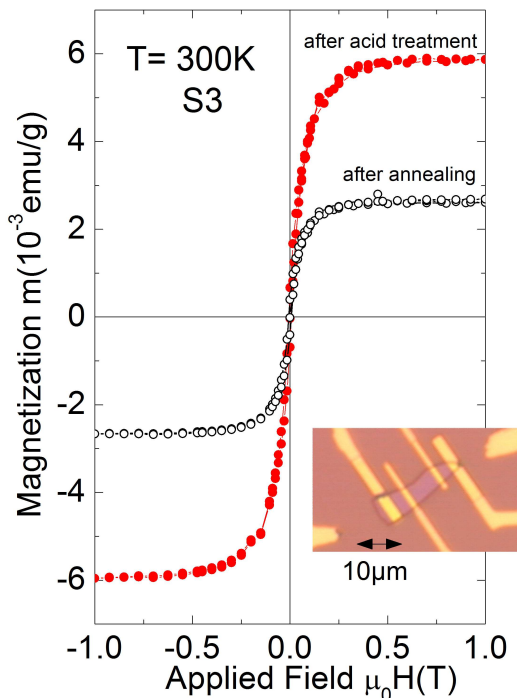


FIG. 3. Magnetization vs. applied magnetic field for sam S3 after acid treatment and after annealing two hours in *v* uum at 250°C. The inset shows an optical microscope pict of the measured graphite flake with the contact Au electrodes.

is measured after diluted acid treatment. The sample was treated with an acid droplet, similar to that used for sample S3. This amplitude can be compared to $\simeq 0.6\%$ obtained for a pure Co polycrystalline film of size $0.6 \times 0.38 \text{ mm}^2$ and 12 nm thickness, see Fig. 4. Assuming that ~ 2 nm from the treated graphite flake becomes ferromagnetic after the acid treatment and that the bulk of the sample does not contribute to the AMR, a simple parallel resistor model indicates that the real AMR amplitude of the ferromagnetic near surface region should be at least 20 times larger, i.e. in the 2% range. The amplitude of the AMR increases decreasing temperature as the data obtained at 30 K indicate, see Fig. 4. In ferromagnetic materials with elements with *d*-bands the AMR effect is attributed to the larger probability for a *s* – *d* scattering of electrons moving parallel to the applied field. Its origin is related to: (1) the spin asym-

metry of the *d*-band and (2) to a finite *L* – *S* coupling, which allows electrons to have a spin-flip, enhancing in this way the scattering probability and therefore the resistance. As pointed out in Ref. 16 the fact that magnetic graphite shows the AMR phenomenon indicates both, a non-negligible *L* – *S* coupling and a spin splitting of the *p*-band. Although for carbon-based systems a negligible *L* – *S* coupling is expected due to the low atomic number

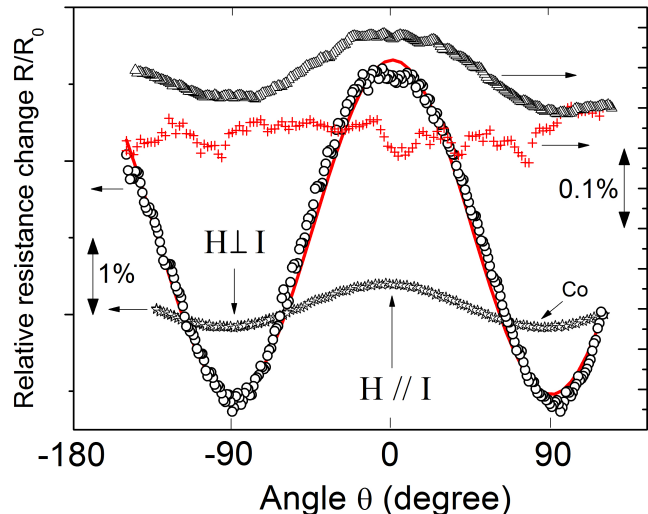


FIG. 4. Relative change of the electrical resistance vs. the angle between the magnetic field ($\mu_0 H = 0.5 \text{ T}$) and the applied current for the graphite flake at 300 K before (+, right *y*-axis) and after acid treatment (Δ , right *y*-axis). (\circ): data obtained after acid treatment at 30 K under same conditions (left *y*-axis). The continuous line follows the $\cos^2(\theta)$ function, usual for the AMR of polycrystalline magnetic samples. For comparison the AMR measured in a Co polycrystalline film at 300 K is also shown (\star , left *y*-axis).

gen bonding. The results shown in Fig. 4 indicate in fact a giant AMR for hydrogen-mediated magnetic graphite, an effect that supports the XMCD results of Ref. 3.

One of the authors (P.E.) acknowledges discussions with Prof. Dr. S. Penadés (CIC biomaGUNE, San Sebastian). This work is supported by the Deutsche Forschungsgemeinschaft under contract DFG ES 86/16-1. A.B. and S.D. are supported by the Graduate School of Natural Sciences “BuildMoNa” of the University of Leipzig.

* esquin@physik.uni-leipzig.de

† Present address: Helmholtz Centre for Environmental Research-UFZ, Permoserstr 15, D-04318 Leipzig, Germany

¹ For a review see: O. V. Yazyev, Rep. Prog. Phys. **73**, 056501 (2010).

² H. Ohldag, T. Tyliczszak, R. Höhne, D. Spemann, P. Esquinazi, M. Ungureanu, and T. Butz, Phys. Rev. Lett. **98**, 187204 (2007).

³ H. Ohldag, P. Esquinazi, E. Arenholz, D. Spemann, M. Rothermel, A. Setzer, and T. Butz, New Journal of

- Physics **12**, 123012 (2010).
- ⁴ P. Esquinazi, A. Setzer, R. Höhne, C. Semmelhack, Y. Kopelevich, D. Spemann, T. Butz, B. Kohlstrunk, and M. Lösche, Phys. Rev. B **66**, 024429 (2002).
- ⁵ H. Xia, W. Li, Y. Song, X. Yang, X. Liu, M. Zhao, Y. Xia, C. Song, T.-W. Wang, D. Zhu, J. Gong, and Z. Zhu, Adv. Mater. **20**, 4679 (2008).
- ⁶ X. Yang, H. Xia, X. Qin, W. Li, Y. Dai, X. Liu, M. Zhao, Y. Xia, S. Yan, and B. Wang, Carbon **47**, 1399 (2009).
- ⁷ M. A. Ramos, J. Barzola-Quiquia, P. Esquinazi, A. Muñoz Martín, A. Climent-Font, and M. García-Hernández, Phys. Rev. B **81**, 214404 (2010).
- ⁸ E. J. Duplock, M. Scheffler, and P. J. D. Lindan, Phys. Rev. Lett. **92**, 225502 (2004).
- ⁹ K. Potzger, S. Zhou, J. Grenzer, M. Helm, and J. Fassbender, Appl. Phys. Lett. **92**, 182504 (2008).
- ¹⁰ M. Khalid, M. Ziese, A. Setzer, P. Esquinazi, M. Lorenz, H. Hochmuth, M. Grundmann, D. Spemann, T. Butz, G. Brauer, W. Anwand, G. Fischer, W. A. Adeagbo, W. Hergert, and A. Ernst, Phys. Rev. B **80**, 035331 (2009).
- ¹¹ Y. Liu, G. Wang, S. Wang, J. Yang, L. Chen, X. Qin, B. Song, B. Wang, and X. Chen, Phys. Rev. Lett. **106**, 087205 (2011).
- ¹² N. Parkanskya, B. Alterkopa, R. L. Boxmana, G. Leitusb, O. Berkhc, Z. Barkayd, Y. Rosenberg, and N. Eliaz, Carbon **46**, 215 (2008).
- ¹³ J. Barzola-Quiquia, J.-L. Yao, P. Rödiger, K. Schindler, and P. Esquinazi, phys. stat. sol. (a) **205**, 2924 (2008).
- ¹⁴ R. M. Silverstein, G. C. Bassler, and T. C. Morrill, *Spectrometric Identification of Organic Compounds*, Vol. 4 (John Wiley and Sons, 1981).
- ¹⁵ M. D. Obradovic, G. D. Vukovic, S. I. Stevanovic, V. V. Panic, P. S. Uskokovic, A. Kowal, and S. L. Gojkovic, J. Electroanal. Chem. **634**, 22 (2009).
- ¹⁶ P. Esquinazi, J. Barzola-Quiquia, D. Spemann, M. Rothermel, H. Ohldag, N. García, A. Setzer, and T. Butz, J. Magn. Magn. Mat. **322**, 1156 (2010).